

Decyl-End-Capped Thiophene–Phenylene Oligomers as Organic Semiconducting Materials with Improved Oxidation Stability

Sergei A. Ponomarenko,[†] Stephan Kirchmeyer,^{*‡} Andreas Elschner,[‡] Ninel M. Alpatova,[‡] Marcus Halik,[§] Hagen Klauk,[§] Ute Zschieschang,[§] and Günter Schmid[§]

N. S. Enikolopov Institute of Synthetic Polymer Materials of Russian Academy of Sciences, Profsoyuznaya Street 70, Moscow 117393, Russia, H. C. Starck, Research Electronic Chemicals, Central Research and Development Division, Bayerwerk B202, 51368 Leverkusen, Germany, A. N. Frumkin Institute of Electrochemistry of Russian Academy of Sciences, Leninsky Prospect 31, 119071 Moscow, Russia, and Infineon Technologies AG, Polymer Materials and Technology, Paul-Gossen-Strasse 100, 91052 Erlangen, Germany

Received October 5, 2005. Revised Manuscript Received November 9, 2005

The efficient synthesis of decyl-end-capped thiophene–phenylene oligomers with different numbers and positions of 1,4-phenyl rings within a 2,5-oligothiophene conjugated chain, leading to electronic-grade pure semiconducting organic materials with improved oxidation stability, was elaborated. These are p-type organic semiconductors, showing high charge-carrier mobilities up to 0.4 cm²/Vs and on/off current ratios as large as 10⁵ in organic thin-film transistors, as well as stage delays as low as 300 μs in the integrated circuits (ring oscillators). Long decyl end chains in these oligomers having 5–7 conjugated aromatic rings lead to limited solubility but improve the oligomers' crystallinity, making them promising semiconducting materials for organic electronic devices prepared by vapor evaporation. Investigation of the optical properties of the oligomers showed that they have a HOMO–LUMO energy gap approximately 0.2 eV higher than that of the corresponding oligothiophenes. Electrochemical measurements revealed a better oxidation stability of the thiophene–phenylene oligomers as compared to that of their oligothiophene analogues.

Introduction

There has been growing interest in π -conjugated polymers and oligomers over the last few years because of their unique semiconducting and electrooptical properties and potential applications in different electronic devices, such as organic thin-film transistors (OTFTs) and organic light-emitting diodes (OLEDs).^{1,2} By now the major characteristics of organic semiconductors—mobilities of charge carriers—have outperformed the value of amorphous silicon (~ 0.5 cm²/Vs), i.e., 8 cm²/Vs for rubrene,³ 3–5 cm²/Vs for pentacene,^{4,5} 2.4 cm²/Vs for dithiophene–tetrathiafulvalene,⁶ 1.0–1.1 cm²/Vs for α,α' -dialkyloligothiophenes,⁷ and 0.66 cm²/Vs for

thiophene–phenylene co-oligomers.⁸ The most important is that such high mobility values were measured not only for single-crystal devices^{3,6,8} but also for some thin-film devices.^{4,7} It indicates that these organic semiconductors can really be used in the industry for large-scale production of the so-called printed electronics. A prerequisite for high mobility in thin-film devices is a high order of organic semiconductors' molecules in the semiconducting layer,¹ as well as a high purity of the semiconducting material.⁹ However, now more and more attention is paid to the environmental stability of organic semiconductors and devices based on them.^{10,11} Nowadays one can see the trend of having more stable organic semiconductors with a slightly decreased mobility rather than vice versa. This work describes a rational design and systematic study of organic semiconductors with improved oxidation stability based on decyl-end-capped thiophene–phenylene oligomers. It follows

* To whom correspondence should be addressed. Phone: (049) 214 30 72626. Fax: (049) 214 30 25973. E-mail: stephan.kirchmeyer@hcestarck.com.

[†] N. S. Enikolopov Institute of Synthetic Polymer Materials of Russian Academy of Sciences.

[‡] H. C. Starck.

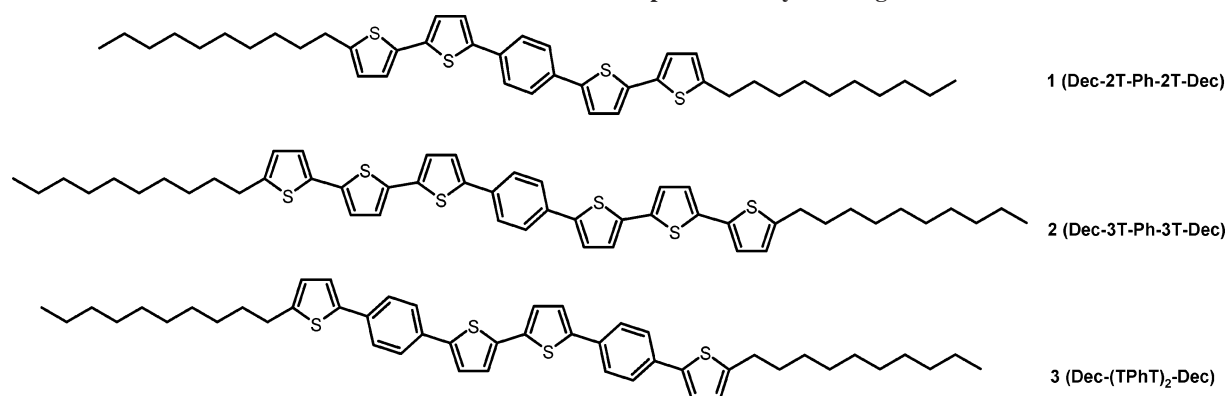
[§] A. N. Frumkin Institute of Electrochemistry of Russian Academy of Sciences.

[§] Infineon Technologies AG.

- (1) (a) Dimitrakolopoulos, C. D.; Malenfant, P. R. L. *Adv. Mater.* **2002**, *14*, 99. (b) Horowitz, G. *Adv. Mater.* **1998**, *10*, 365. (c) Katz, H. E. *J. Mater. Chem.* **1997**, *7*, 369. (d) Katz, H. E. *Chem. Mater.* **2004**, *16*, 4748.
- (2) (a) Bernius, M. T.; Inbasekaran, M.; O'Brien, J.; Wu, W. *Adv. Mater.* **2000**, *12*, 1737. (b) Friend, R. H.; Gymer, G. W.; Holmes, A. B.; Burroughes, J. H.; Marks, R. N.; Taliani, C.; Bradley, D. D. C.; Dos Santos, D. A.; Brédas, J. L.; Lögdlund, M.; Salaneck, W. R. *Nature* **1999**, *397*, 121.
- (3) Podzorov, V.; Sysoev, S. E.; Loginova, E.; Pudalov, V. M.; Gershenson, M. E. *Appl. Phys. Lett.* **2003**, *83*, 3504.
- (4) Klauk, H.; Halik, M.; Zschieschang, U.; Schmidt, G.; Radlik, W.; Weber, W. *J. Appl. Phys.* **2002**, *92*, 5259.
- (5) Kelley, T. W.; Muires, D. V.; Baude, P. F.; Smith, T. P.; Jones, T. D. *Mater. Res. Soc. Symp. Proc.* **2003**, *771*, 651.

- (6) Mas-Torrent, M.; Durkut, M.; Hadley, P.; Ribas, X.; Rovira, C. *J. Am. Chem. Soc.* **2004**, *126*, 984.
- (7) (a) Halik, M.; Klauk, H.; Zschieschang, U.; Schmid, G.; Ponomarenko, S.; Kirchmeyer, S.; Weber, W. *Adv. Mater.* **2003**, *15*, 917. (b) Halik, M.; Klauk, H.; Zschieschang, U.; Schmid, G.; Ponomarenko, S.; Kirchmeyer, S. *Mater. Res. Soc. Symp. Proc.* **2003**, *771*, 321.
- (8) Ichikawa, M.; Yanagi, H.; Shimizu, Y.; Hotta, S.; Suganuma, N.; Koyama, T.; Taniguchi, Y. *Adv. Mater.* **2002**, *14*, 1272.
- (9) Katz, H. E.; Bao, Z.; Gilat, S. L. *Acc. Chem. Res.* **2001**, *34*, 359.
- (10) (a) Meng, H.; Bao, Z.; Lovinger, A. J.; Wang, B.-C.; Mujsce, A. M. *J. Am. Chem. Soc.* **2001**, *123*, 9214. (b) Meng, H.; Zheng, J.; Lovinger, A. J.; Wang, B.-C.; van Patten, P. G.; Bao, Z. *Chem. Mater.* **2003**, *15*, 1778.
- (11) Ong, B. S.; Wu, Y.; Liu, P.; Gardner, S. *J. Am. Chem. Soc.* **2004**, *126*, 3378.

Scheme 1. Chemical Structures of Thiophene–Phenylene Oligomers 1–3



our previous investigations, in which we showed that decyl-end-capped α,α' -oligothiophenes have significant molecular ordering effects induced by the long decyl end groups,¹² leading to improved electrical characteristics.¹³

The first examples of thiophene–phenylene oligomers were reported in 1999–2000 by Hotta et al.¹⁴ Because of their unique properties, these materials may be useful as light-emitting layers in OLEDs and organic laser diodes,¹⁵ as well as semiconducting materials for OTFTs.¹⁶ The synthesis and application of other examples of thiophene–phenylene oligomers for OTFTs were recently presented by Katz et al.,¹⁷ Facchetti,¹⁸ and Frisbie et al.¹⁹ However, they used either shorter alkyl end chains or other combinations of the phenyl and thienyl rings in the conjugated oligomer, thus obtaining mobility values up to 0.02–0.09 cm²/Vs. The present work reports on the following: (i) efficient synthesis of a series of decyl-end-capped thiophene–phenylene oligomers **1–3** (Scheme 1) with different numbers and positions of 1,4-phenyl rings within a 2,5-oligothiophene conjugated chain; (ii) comparison of thermal, optical, and electrochemical characteristics of the thiophene–phenylene oligomers and their oligothiophene analogues; (iii) fabrication and electrical characterization of OTFTs and integrated circuits based on the synthesized oligomers, with mobilities as large as 0.4 cm²/Vs, on/off current ratios as large as 10⁵, and signal delays as low as 300 μ s (measured with ring oscillators).

Experimental Section

General. The ¹H NMR spectra were recorded using a Bruker DPX 400 spectrometer equipped with a QNP probe head operating at 400.13 MHz for ¹H in CDCl₃ solutions unless otherwise mentioned.

The phase transitions were studied by means of differential scanning calorimetry (DSC) using a Mettler TA-4000 thermosystem at scanning rates of 10 and 1 K/min. Sample weights were typically chosen between 5 and 10 mg.

Fluorescence Measurements. Dilute solutions of the oligomers in CHCl₃ were prepared to obtain absorption, excitation, and emission spectra. The extinction of the solution in the case of excitation and emission spectra was set to about $E = 0.05$ in a 10 mm quartz cuvette to avoid reabsorption. The absorption spectra were recorded with a Perkin-Elmer 900 spectrometer including a light-integrating sphere, whereas the excitation and emission spectra were recorded with an Edinburgh FL900 spectrometer with a 0°/90° excitation-detection geometry in the cw-mode. The excitation energies were set to the maxima of the excitation spectra.

Cyclic Voltammetry Measurements. Solid compact layers of the oligomers were made by electrostatically rubbing the materials onto a Pt electrode (0.03 cm²). Measurements were made in 0.1 M Bu₄NBF₄ solutions in acetonitrile at different scan rates (25–200 V/s) with a potentiostat–galvanostat IPC-4M.

Materials. Anhydrous THF, MgBr₂·Et₂O complex, Pd(dppf)Cl₂·CH₂Cl₂ complex,²⁰ *n*-butyllithium in hexane, 1,4-dibromobenzene, diethyl ether, 1 N hydrochloric acid, 2-isopropoxy-4,4,5,5-tetramethyl-1,3,2-dioxaborolane (IPTMDOB), and diisopropylamine were purchased from Sigma-Aldrich Co., and were used without further purification. The synthesis and characterization of 2-bromo-5-decylthiophene, 5-decyl-2,2'-bithiophene, and 5-decyl-2,2':5',5''-terthiophene (**4**) are described elsewhere.¹² All glassware was dried before the reaction in a drybox at 100 °C overnight, assembled while hot, and cooled in a stream of nitrogen.

5-Decyl-5'-[4-(5'-decyl-2,2'-bithien-5-yl)phenyl]-2,2'-bithiophene (1**)** was obtained as described elsewhere.²¹ ¹H NMR (300 MHz, C₂D₂Cl₄, TMS, δ): 0.88 (t, 6H, $J = 7.0$ Hz), 1.20–1.45 (overlapped peaks, 28H), 1.68 (m, 4H), 2.79 (t, 4H, $J = 7.5$ Hz), 6.68 (d, 2H, $J = 3.6$ Hz), 6.97 (d, 2H, $J = 3.6$ Hz), 6.99 (d, 2H, $J = 3.6$ Hz), 7.04 (d, 2H, $J = 3.6$ Hz), 7.05 (s, 2H). EI-MS: m/e 686 (M^{+} , 100%).

- (12) Ponomarenko, S.; Kirchmeyer, S. *J. Mater. Chem.* **2003**, *13*, 197.
- (13) Halik, M.; Klauk, H.; Zschieschang, U.; Schmid, G.; Radlik, W.; Ponomarenko, S.; Kirchmeyer, S.; Weber, W. *J. Appl. Phys.* **2003**, *93*, 2977.
- (14) (a) Hotta, S.; Lee, S. A. *Synth. Met.* **1999**, *101*, 551. (b) Hotta, S.; Lee, S. A.; Tamaki, T. *J. Heterocycl. Chem.* **2000**, *37*, 25. (c) Hotta, S.; Kimura, H.; Lee, S. A.; Tamaki, T. *J. Heterocycl. Chem.* **2000**, *37*, 281.
- (15) (a) Lee, S. A.; Yoshida, Y.; Fukuyama, M.; Hotta, S. *Synth. Met.* **1999**, *106*, 39. (b) Yanagi, H.; Morikawa, T.; Hotta, S.; Yase, K. *Adv. Mater.* **2001**, *13*, 313. (c) Hibino, R.; Nagawa, M.; Hotta, S.; Ichikawa, M.; Koyama, T.; Taniguchi, Y. *Adv. Mater.* **2002**, *14*, 119.
- (16) (a) Ichikawa, M.; Yanagi, H.; Shimizu, Y.; Hotta, S.; Suganuma, N.; Koyama, T.; Taniguchi, Y. *Adv. Mater.* **2002**, *14*, 1272. (b) Yanagi, H.; Araki, Y.; Ohara, T.; Hotta, S.; Ichikawa, M.; Taniguchi, Y. *Adv. Funct. Mater.* **2003**, *13*, 767.
- (17) Hong, X. M.; Katz, H. E.; Lovinger, A. J.; Wang, B.-C.; Raghavachari, K. *Chem. Mater.* **2001**, *13*, 4686.
- (18) (a) Mushrush, M.; Facchetti, A.; Lefenfeld, M.; Katz, H. E.; Marks, T. J. *J. Am. Chem. Soc.* **2003**, *125*, 9414. (b) Facchetti, A.; Letizia, J.; Yoon, M.-H. J.; Mushrush, M.; Katz, H. E.; Marks, T. J. *Chem. Mater.* **2004**, *16*, 4715.
- (19) Mohapatra, S.; Holmes, B. T.; Newman, C. R.; Prendergast, C. F.; Frisbie, C. D.; Ward, M. D. *Adv. Funct. Mater.* **2004**, *14*, 605.

- (20) 1,1'-Bis(diphenylphosphino)ferrocene dichloropalladium(II) complexed with dichloromethane (1:1).
- (21) Ponomarenko, S. A.; Kirchmeyer, S.; Halik, M.; Klauk, H.; Zschieschang, U.; Schmid, G.; Karbach, A.; Drechsler, D.; Alpatova, N. *Synth. Met.* **2005**, *149*, 231.
- (22) Obtained using a Varian Unity 300 spectrometer, equipped with a 4Nuc probehead operating at 300.29 MHz for ¹H at 90 °C.

2-(5''-Decyl-2,2':5',2''-terthien-5-yl)-4,4,5,5-tetramethyl-1,3,2-dioxaborolane (5). *n*-Butyllithium (2.5 M in hexane, 2.4 mL, 6.0 mmol) was added to absolute THF (30 mL) at -78°C under nitrogen. A solution of 5-decyl-2,2':5',5''-terthiophene (2.33 g, 6.0 mmol) in dry THF (50 mL) was then added dropwise. The reaction mixture was stirred for 1 h at -78°C ; the bath was then removed, and the temperature was allowed to rise to 10°C . After that, the reaction mixture was cooled again to -78°C , and 2-isopropoxy-4,4,5,5-tetramethyl-1,3,2-dioxaborolane (1.30 g, 1.4 mL, 7.0 mmol) was added in one portion via syringe. The mixture was stirred for 30 min at -78°C ; the bath was then removed, and the mixture was stirred for an additional 3 h while the temperature increased slowly to 23°C . After that, the reaction mixture was poured into 300 mL of ether, and then 100 mL of ice–water mixed with 7 mL of 1 M HCl. The organic phase was separated, washed with water, dried over sodium sulfate, and evaporated to yield the product as a green solid. The product was then used for the next reactions without purification. Yield: 3.02 g (98%). ^1H NMR (CDCl_3 , TMS, δ): 0.88 (3H, t, $J = 6.9$ Hz), 1.20–1.45 (overlapped peaks, 14H), 1.35 (s, 12H), 1.68 (2H, m, $J = 7.5$ Hz), 2.79 (2H, t, $J = 7.6$ Hz), 6.68 (1H, d, $J = 3.4$ Hz), 6.99 (2H, dd, $J_1 = 3.9$ Hz, $J_2 = 3.9$ Hz), 7.11 (1H, d, $J = 3.9$ Hz), 7.21 (1H, d, $J = 3.9$ Hz), 7.52 (1H, d, $J = 3.4$ Hz). EI-MS: m/e 514 (M^+ , 90%).

5-Decyl-5''-[4-(5''-decyl-2,2':5',2''-terthien-5-yl)phenyl]-2,2':5',2''-terthiophene (2). A 100 mL three-necked flask equipped with a magnetic stirring bar, condenser, nitrogen-inlet, and septum was charged with 1,4-dibromobenzene (142 mg, 0.6 mmol), filled with nitrogen, put into a nitrogen-filled drybox, and charged with $\text{Pd}(\text{PPh}_3)_4$ (46 mg, 0.04 mmol). The glassware was assembled and removed from the drybox. Solutions of compound **5** (865 mg, 1.68 mmol) in 20 mL of toluene and 5 mL of 2 M sodium carbonate (aq) were prepared and deoxygenated with a stream of nitrogen. These solutions were added to the reaction vessel, and the mixture was heated to boiling. After 2 h of heating, an orange precipitate appeared. The reaction mixture was refluxed overnight. It was then cooled to rt and poured into a flask containing 100 mL of water mixed with 20 mL of 1 M HCl and 200 mL of toluene. The aqueous and organic phases were separated, and the organic phase, containing the product as a precipitate, was washed with water and filtered over glass filter G4. The product was washed with toluene and dried under vacuum (0.1 mbar) to give 404 mg of a thin orange powder, which was already 99% pure according to EI-MS. Yield: 404 mg (79%). The product was further purified by sublimation. EI-MS: m/e 850 (M^+ , 100%).

1-Thienyl-4-bromobenzene (6). Under nitrogen, a solution of 2-bromothiophene (8.56 g, 52.5 mmol) in anhydrous diethyl ether (45 mL) was slowly added dropwise to a suspension of magnesium (1.32 g, 55 mmol) in anhydrous diethyl ether (5 mL). The corresponding Grignard reagent was refluxed for 2 h, cooled to room temperature, and transferred to the dropping funnel of the second apparatus via syringe. It was added dropwise to a solution of 1,4-dibromobenzene (11.80 g, 50 mmol) and $\text{Pd}(\text{dppf})\text{Cl}_2\cdot\text{CH}_2\text{Cl}_2$ complex (366 mg, 0.5 mmol) in 50 mL of anhydrous ether. The reaction temperature increased from 20 to 34°C . The mixture was stirred overnight, while the temperature decreased to 20°C again. Completeness of the reaction was controlled by TLC in 4:1 hexane–chloroform. The reaction mixture was then hydrolyzed with 1 N HCl (10 mL), poured into 100 mL of ice–water, and extracted twice with 300 mL of ether. The combined ether layers were washed with water, dried over sodium sulfate, and evaporated to give the raw product, which according to GC–MS contained 1-thienyl-4-bromobenzene (64.57%), 1,4-dibromobenzol (18.14%), and 1,4-bithienylbenzol (17.29%). The raw product was purified by recrystallization from hexane followed by column chromatography

in silica gel to yield 4.21 g of 99% pure (GC–MS) product as white crystals. Reaction yield: 64%. Isolated yield: 35%. NMR (CDCl_3 , TMS, δ): 7.07 (t, 1H, $J = 4.4$ Hz), 7.29 (d, 2H, $J = 4.4$ Hz), 7.48 (d, 4H, $J = 3.4$ Hz).

1-(Thien-2'-yl)-4-(5''decyl-thien-2''-yl)benzene (7). Under nitrogen, a solution of 2-bromo-5-decylthiophene (6.37 g, 21 mmol) in anhydrous diethyl ether (30 mL) was slowly added dropwise to a suspension of magnesium (530 mg, 22 mmol) in anhydrous diethyl ether (5 mL). The Grignard reaction started with the help of a few drops of 1,2-dibromoethane. The reaction mixture was refluxed for 5 h, cooled to room temperature, and transferred to the dropping funnel of the second apparatus via syringe. It was added dropwise to solution of 1-thienyl-4-bromobenzene (**6**) (4.2 g, 18 mmol) and $\text{Pd}(\text{dppf})\text{Cl}_2\cdot\text{CH}_2\text{Cl}_2$ complex (140 mg, 0.2 mmol) in anhydrous diethyl ether (30 mL). During dropping, the temperature increased from 15 to 28°C , and the product precipitated. The reaction mixture was then stirred overnight at 23°C . Completion of the reaction was controlled by TLC in hexane. The reaction mixture was hydrolyzed dropwise with 10 mL of 1 N HCl, immediately poured into 200 mL of water, and extracted with diethyl ether. The combined layers, containing the product as a precipitate, were washed with water and filtered over glass filter G2 to get 5.61 g of white-greenish crystals. The raw product was purified by recrystallization from chloroform. Yield: 4.83 g (72%). ^1H NMR (CDCl_3 , TMS, δ): 0.88 (t, 3H, $J = 7.1$ Hz), 1.20–1.45 (overlapped peaks with max at 1.270, 14H), 1.70 (m, 2H, $J = 7.3$ Hz), 2.82 (t, 2H, $J = 7.6$ Hz), 6.75 (d, 1H, $J = 3.4$ Hz), 7.08 (dd, 1H, $J_1 = 5.1$ Hz, $J_2 = 3.7$ Hz), 7.15 (d, 1H, $J = 3.9$ Hz), 7.27 (dd, 1H, $J_1 = 1.0$ Hz, $J_2 = 4.9$ Hz), 7.32 (dd, 1H, $J_1 = 1.0$ Hz, $J_2 = 3.4$ Hz), 7.57 (dd, 4H, $J_1 = 15.2$ Hz, $J_2 = 8.3$ Hz).

5,5'-Bis[4-(5-decyl-2-thienyl)phenyl]-2,2'-bithiophene (3). *n*-Butyllithium (2.5 M in hexane, 0.8 mL, 2.0 mmol) was added to absolute THF (20 mL) at -78°C under nitrogen. A solution of diisopropylamine (223 mg, 2.2 mmol) in absolute THF (10 mL) was then added in one portion. A bath with acetone–dry ice was then replaced with another bath containing NaCl–ice. When the temperature increased to -40°C , a solution of 1-(thien-2'-yl)-4-(5''-decyl-thien-2''-yl)benzene (**7**) (766 mg, 2.0 mmol) in 30 mL of absolute THF was added dropwise. Almost from the beginning of dropping, the solution became turbid, and white precipitate then appeared. The solution became blue, then dark-green, and finally brown. The bath was removed, and the temperature was allowed to rise to 10°C . Complete dissolving of the precipitate happened at $\sim 5^{\circ}\text{C}$, forming a dark brown solution. After that, the reaction mixture was cooled again to -78°C , and anhydrous powdered CuCl_2 (538 mg, 4.0 mmol) was added in one portion. The color of the solution changed from brown to green. The dry ice–acetone bath was removed; the temperature increased to 22°C , and the reaction mixture was stirred for 2 h. It was then poured into 200 mL of ether and 200 mL of ice–water mixed with 10 mL of 1 N HCl. The ether layer, containing a yellow-greenish precipitate, was separated, washed with water, filtered off, and washed with dry ether. The precipitate was dried in a vacuum (0.1 mbar) to constant weight to give 223 mg of the product as a light green solid. Yield: 223 mg (29%). The product was further purified by sublimation to give a yellow solid. EI-MS: m/e 762 (M^+ , 100%).

Results and Discussion

Synthesis. Oligomers **1** and **2** with an odd number of aromatic rings were designed to have one *p*-phenylene unit between the oligothiophene blocks of different lengths (bi- and terthiophenes, respectively). On the one hand, it allows for direct comparison with their oligothiophene analogues

Scheme 2. Synthesis of Thiophene–Phenylene Oligomers 1–3

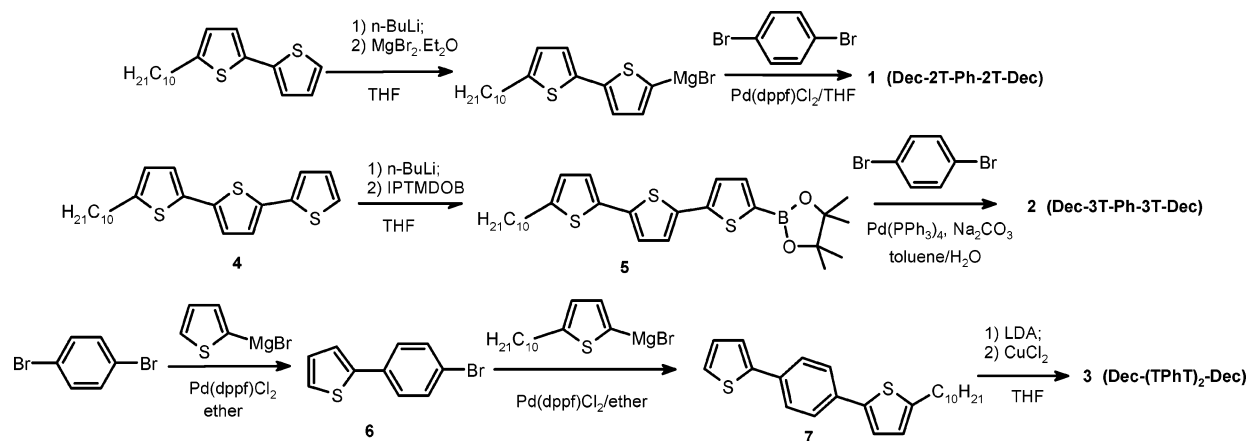


Table 1. Phase Behavior of Oligomers Obtained

compd	T_m (°C)	melting enthalpy (kJ mol ⁻¹)
1	K1 109 K2 124 K3 212 SmX 253 I	K1 28.8 K2 17 K3 23 SmX 19.2 I
2	K 311 I	K 36.6 I
3	K 316 SmX 351 I	K 30.8 SmX 24.1 I

^a K1, K2, and K3 are different crystal phases, SmX is an undefined smectic phase, and I is an isotropic melt.

α,α' -didecyloligothiophenes.¹² On the other hand, they are linear analogues of the semiconducting star-shaped oligomers with the central 1,3,5-phenyl ring²³ that makes it possible to trace the influence of the way the oligothiophene blocks are connected to the phenyl ring on the properties of the oligomers obtained. Oligomer **3** was designed in such a way as to have a structure similar to that of α,α' -didecylsexithiophene, but with the second and fourth thienyl rings replaced with 1,4-linked phenyl rings.

The thiophene–phenylene oligomers were synthesized as depicted in Scheme 2. The most efficient procedure was found for 1,4-bis(5-decyl-2,2'-bithien-5-yl)benzene (**1**). In this case, the use of Pd(dppf)Cl₂ as a catalyst for Kumada coupling of 5-decyl-2,2'-bithien-5-ylmagnesium bromide to 1,4-dibromobenzene led to such a high purity of oligomer **1** that it was used for the fabrication of OTFTs without any additional purification.²¹ However, this approach was found to not be universal, and our attempts to synthesize pure 1,4-bis(5-decyl-2,2':5',2''-terthien-5''-yl)benzene (**2**) from 5-decyl-2,2':5',2''-terthien-5''-ylmagnesium bromide and 1,4-dibromobenzene using a similar procedure failed, producing a significant amount of a byproduct, α,α' -didecylsexithiophene. Consequently, Suzuki coupling was used to prepare oligomer **2**. Thanks to the nature of the Suzuki coupling reaction, and with the proper choice of halogen and boronic compounds, we were able to obtain the desired oligomer **2** with high purity after simple sublimation. It is well-known that the electrical performance of OTFTs depends critically on the purity of the organic semiconductor; it is particularly sensitive to the presence of oligomers with mismatched lengths.²⁴ The relatively poor stability of the thiophene boronic acid derivatives, which decrease with an increase in the number of thienyl units,²⁵ was improved dramatically through the use of pinacolone ester of the boronic acid derivative, which is known to form more stable organoboronic aromatic

compounds.²⁶ Oligomer **3** was synthesized by the oxidative coupling of 1-(thien-2'-yl)-4-(5''-decyl-thien-2''-yl)benzene (**7**), a synthesis similar to that of α,α' -didecylsexithiophene (**Dec-6T-Dec**) described earlier.¹² Precursor **7** was obtained via a repetitive Kumada coupling of 2-thienylmagnesium bromide followed by 5-decyl-2-thienylmagnesium bromide to 1,4-dibromobenzene with the isolation and purification of intermediate compound **6**.

The structure and purity of the intermediate and final compounds were proved by ¹H NMR spectroscopy, GC–MS, and EI-MS analysis. All three final thiophene–phenylene oligomers obtained possess a very limited solubility even in hot solvents, thus prohibiting their processing from the liquid phase. This is in sharp contrast to their star-shaped analogues, which possess good solubility and film-forming properties, leading to an improved spin-coating processing.²³ Nevertheless, the solubility of oligomers **1–3** in chlorinated solvents was enough to investigate their optical properties. A possible reason for the low solubility of the oligomers in question is the strong interactions between the aromatic units of the molecules in the solid state, increased by the additional interactions between the long decyl end groups of the molecules.

Thermal Properties. The thermal behavior of the thiophene–phenylene oligomers synthesized was characterized by polarizing optical microscopy and differential scanning calorimetry (DSC) methods (Table 1).

These investigations revealed a high crystallinity of all the materials obtained. Compounds **1** and **3** possess not only crystalline but also high-temperature liquid crystalline mes-

(23) Ponomarenko, S. A.; Kirchmeyer, S.; Elschner, A.; Huisman, B.-H.; Karbach, A.; Drechsler, D. *Adv. Funct. Mater.* **2003**, *13*, 591.

(24) Katz, H. E.; Dodabalapur, A.; Bao Z. In *Handbook of Oligo- and Polythiophenes*; Fichou, D., Ed.; Wiley-VCH: Weinheim, Germany, 1999; p 459.

(25) Tsvigoulis, G. M.; Lehn, J.-M. *Chem.–Eur. J.* **1996**, *11*, 1399.

(26) (a) Bidan, G.; de Nicola, A.; Enée, V.; Guillerez, S. *Chem. Mater.* **1998**, *10*, 1052. (b) Guillerez, S.; Bidan, G. *Synth. Met.* **1998**, *93*, 123. (c) Kirschbaum, T.; Briehn, C. A.; Bäuerle, P. *J. Chem. Soc., Perkin Trans. 1* **2000**, 1211. (d) Jayakannan, M.; Dongen, J. L. J.; Janssen, R. A. J. *Macromolecules* **2001**, *34*, 5386.

Table 2.^a UV–Vis Absorption and Fluorescence Data for the Oligomers^a

compd	abs max (nm)	fluorescence max (nm)	HOMO–LUMO gap (eV)
1	401	456, 484	2.81
2	434	496, 532	2.60
3	414	472, 504	2.72
Dec-4T-Dec^b	400	464, 492	2.77
Dec-5T-Dec	421	494, 528	2.61
Dec-6T-Dec	444	517, 554	2.50

^aMeasured in dilute solutions in CHCl₃. ^bMeasured in CH₂Cl₂.

ophases. Bearing in mind rather high isotropization enthalpies (19–24 kJ mol^{−1}) as well as a molecular symmetry, we could attribute these to ordered smectic mesophases, designated here as SmX. Exact determination of the mesophase types demands further examination with XRD measurements. Oligomer **3** shows the highest melting and isotropization temperatures (316 and 351 °C, respectively), whereas oligomer **1** has the highest degree of ordering in the crystalline phase, as can be estimated from the thermodynamic data.¹² As can further be seen, both oligomers showed the highest field-effect mobility, measured until now for thin films of thiophene–phenylene oligomers.

Optical Properties. Investigation of the influence of inclusion of *p*-phenylene rings into conjugated oligothiophene molecules was made by UV–vis absorption and fluorescence measurements in dilute chloroform solutions of thiophene–phenylene oligomers **1–3** (Table 2).

Data for their oligothiophene analogues, namely, α,α′-didecylquaterthiophene (**Dec-4T-Dec**), α,α′-didecylquinquethiophene (**Dec-5T-Dec**), and α,α′-didecylsexithiophene (**Dec-6T-Dec**),¹² are also shown. The HOMO–LUMO energy gap Δ*E* was estimated from the optical measurements as the intersection of the excitation and emission spectra, regarded as mirrors of a 0–0 transition. Such estimation for oligothiophenes usually gives Δ*E* values that coincide well with the energy gap obtained electrochemically.²⁷

Compared with that of **Dec-5T-Dec**, the absorption and emission maxima of 5-ring oligomer **1** in dilute solutions are shifted toward higher energy by 20–40 nm, and they are much closer to those obtained for **Dec-4T-Dec**. The estimated value of the HOMO–LUMO gap for oligomer **1** is 2.81 eV, which is close to the value of 2.77 eV for **Dec-4T-Dec** but 0.2 eV larger than the energy gap for **Dec-5T-Dec** with Δ*E* = 2.61 eV. These results indicate that replacing the central 2,5-thienyl group in α,α′-didecylquinquethiophene with a 1,4-phenylene group leads to an increase in the HOMO–LUMO gap to approximately the value for **Dec-4T-Dec**. In other words, by inserting the 1,4-phenylene group between two bithiophene blocks, we can increase the oligomer length from 4 to 5 conjugated rings without increasing the HOMO–LUMO gap. Data for oligomers **2** and **3** confirm this tendency. The 7-ring thiophene–phenylene oligomer **2** has an energy gap of ca. 2.60 eV, which is actually the same as that of the 5-ring oligothiophene **Dec-5T-Dec**. The difference in the energy gap is even higher for 6-ring thiophene–phenylene oligomer **3** (Δ*E* = 2.72 eV),

Table 3. Electrochemical Data for Thin Films of Oligomers Measured by CV vs SCE

compd	standard formal oxidation potentials		HOMO (eV)
	<i>E</i> _{1f} ⁰ (V)	<i>E</i> _{2f} ⁰ (V)	
1	1.15		−5.55
2	1.18	1.34	−5.58
3	1.25	1.57	−5.65
Dec-4T-Dec	1.01	1.07	−5.41
Dec-5T-Dec	0.99		−5.39
Dec-6T-Dec	1.02	1.18	−5.42

compared with Δ*E* = 2.50 eV for **Dec-6T-Dec**. The energy gap of oligomer **3** is between those for 4- and 5-ring oligothiophenes **Dec-4T-Dec** and **Dec-5T-Dec**, although it's closer to the former. This strong shift is caused by the presence of two *p*-phenylene rings in the conjugated chain of the molecule. Thus, as expected in the linear thiophene–phenylene oligomers, the *p*-phenylene groups do not break the conjugation between the oligothiophene units but do influence their HOMO–LUMO band gap. This is in sharp contrast to star-shaped oligomers, in which a linking of oligothiophene units to a 1,3,5-phenyl ring breaks the conjugation, leading to three independently conjugated oligothiophene–phenylene blocks within one molecule.²³

Cyclic Voltammetry. The peculiarities of the energy levels of linear thiophene–phenylene oligomers, found by optical measurements, should influence their oxidation stability as compared to the oligothiophenes with the same number of aromatic rings. The most interesting question was the electrooxidative stability of these oligomers in thin films, i.e., close to the working conditions of organic semiconductors in OTFTs. This point was tackled with electrochemical measurements of thin films of the thiophene–phenylene oligomers and model oligothiophene compounds (Table 3).

Typical cyclovoltammograms of the thin films of the oligomers investigated are shown in Figure 1. All the oligomers are oxidized quasireversibly. The technique used permits us to obtain CVs practically in only the first cycle, during which the currents markedly decreased. The most probable reason for such behavior is the exfoliation of the films off the electrode surface. The reproducibility was checked by multiple experiments. Usually, oxidation of the oligothiophenes involves two steps: (1) formation of the radical cation and (2) formation of the dication, corresponding to the first and second redox processes with the standard formal potentials *E*_{1f}⁰ and *E*_{2f}⁰, respectively. Sometimes the second redox process could not be seen, especially in the thicker films.²⁸ But because we were interested in the comparison of the oxidation stability of thin films from the oligomers synthesized, the point in question was the first oxidation step, with its standard oxidation potential *E*_{1f}⁰.²⁹

Cyclovoltammetry showed that all three model oligothiophenes, **Dec-4T-Dec**, **Dec-5T-Dec**, and **Dec-6T-Dec**, are oxidized practically at the same standard formal oxidation potentials *E*_{1f}⁰ (Table 3). These are independent of the number of thiophene rings in the oligomer and lie near the value of 1.0 V. At first glance, this result seems to be rather unusual, bearing in mind a lot of publications showing that

(27) Demanze, F.; Cornil, J.; Garnier, F.; Horowitz, G.; Valat, P.; Yassar, A.; Lazzaroni, R.; Bredas, J.-L. *J. Phys. Chem.* **1997**, *101*, 4553.(28) Zotti, G.; Schiavon, G.; Berlin, A.; Pagani, G. *Chem. Mater.* **1993**, *5*, 620.

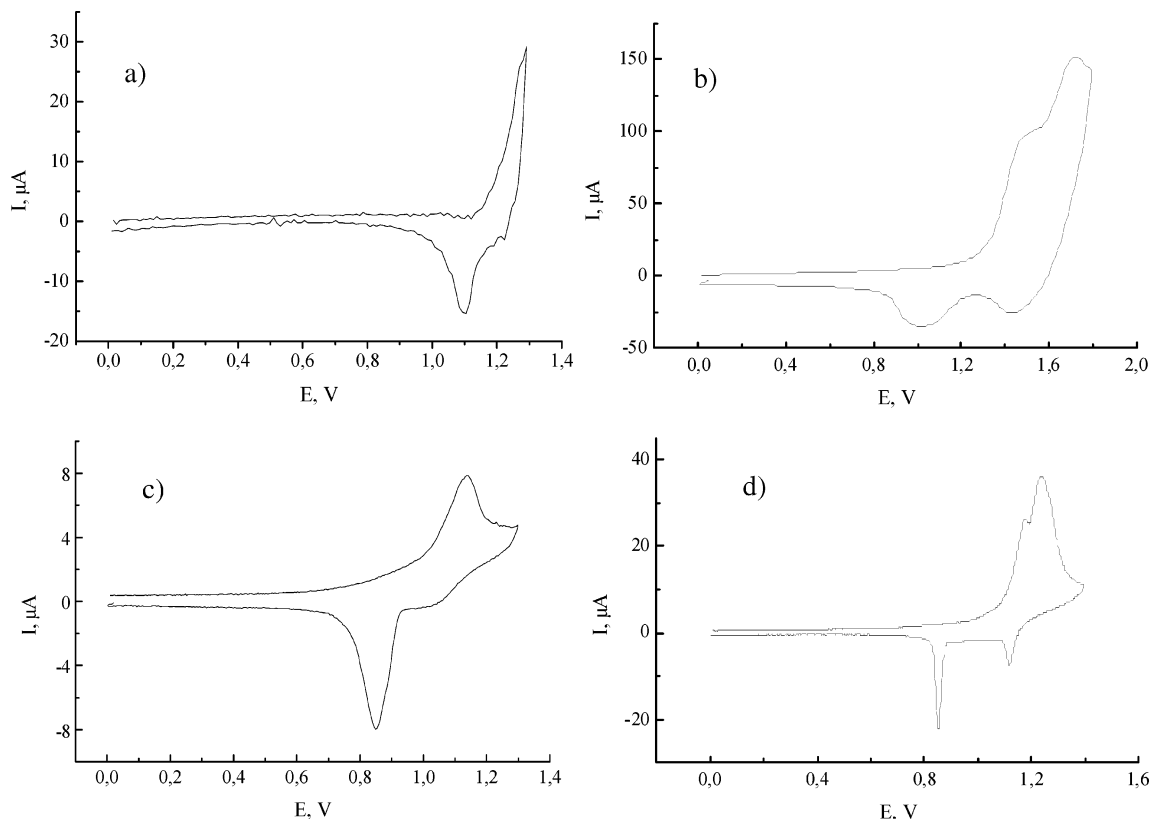


Figure 1. Cyclic voltammograms of thin films recorded in 0.1 M Bu₄NBF₄/AN for (a) thiophene–phenylene oligomer **1**, (b) thiophene–phenylene oligomer **3**, (c) oligothiophene **Dec-5T-Dec**, and (d) oligothiophene **Dec-6T-Dec**.

the oxidation potential decreases with an increase in the length of the oligothiophene.³⁰ For the oligothiophenes with 4–6 thiophene rings, typically the first oxidation potential decreases by 0.05 V with each additional thiophene ring. However, one should keep in mind that these literature data were obtained for dilute solutions of the oligomers, and they reflect only the electronic structure of the molecules. Our goal was to estimate the oxidative stability of thin films of the oligomers. That is why we have made the measurements in solid films, where not only electronic properties of the single molecules but also ordering between the molecules is taken into account. Most probably, the close E_{if}^0 values obtained are a consequence of the interactions between the molecules in the solid-state measurements. CV data of the solid films of methyl-end-capped oligothiophenes with 4, 6, 8, and 10 thiophene rings favor this assumption, showing a much lower difference between their oxidation potentials (the calculated difference between E_{if}^0 of 4-mer and of 10-mer is just 0.1 V).²⁸ It is well known that interactions in the solid state can alter positions of the electronic levels, for instance, because of close contacts of the oligomers' fragments with each other and the formation of stacks or lamellar structures. The higher the ordering in the solid phase, the stronger the interactions of the π -systems between different oligomer's fragments and the easier the process of electron exchange

with the electrode takes place. These processes can change the values of E_{if}^0 . We explain the actual constancy of the formal potential in the raw **Dec-4T-Dec**, **Dec-5T-Dec**, and **Dec-6T-Dec** by compensation of two opposite effects: (1) an increase in the number of conjugated rings in the oligothiophene fragment, which should decrease the potential, and (2) the influence of the ordering in the solid state under the considerable impact of long alkyl chains. One can suppose that the latter effect is stronger the shorter the oligothiophene fragment is. And the higher the ordering, the greater the interactions of the π -systems between the different oligothiophenes are and the easier oxidation is.

For thiophene–phenylene oligomers **1–3**, E_{if}^0 increases with the introduction of *p*-phenylene rings into the oligomers (Table 3). Moreover, introduction of one *p*-phenylene ring into oligothiophene increases its oxidation potential by ca. 0.15 V. Introduction of the second *p*-phenylene ring shifts its oxidation potential further by ca. 0.10 V. It means that all the thiophene–phenylene oligomers are significantly more stable in air than the corresponding oligothiophenes. In increasing order of oxidation potential, the thiophene–phenylene oligomers can be arranged as follows: **1** \approx **2** < **3**. In other words, oligomer **3** with $E_{\text{if}}^0 = 1.25$ has the highest oxidation stability among all the oligomers and oligothiophenes under consideration.

The electrochemical data obtained allowed us to estimate the HOMO levels from the vacuum for the oligomer films (also called their ionization potentials, IPs). For this purpose, the following potentials were taken into account: (1) the HOMO level of the metal electrons at the normal hydrogen electron in water is -4.43 eV,³¹ (2) the potential shift

(29) The formal potentials were calculated as the arithmetic mean between the potentials corresponding to maximum currents of the anodic and cathodic processes.

(30) (a) Xu, Z.; Fichou, D.; Horowitz, G.; Garnier, F. J. *Electroanal. Chem.* **1989**, 267, 339. (b) Baeuerle, P. *Adv. Mater.* **1992**, 4, 102. (c) Facchetti, A.; Mushrush, M.; Katz, H. E.; Marks, T. J. *Adv. Mater.* **2003**, 15, 33.

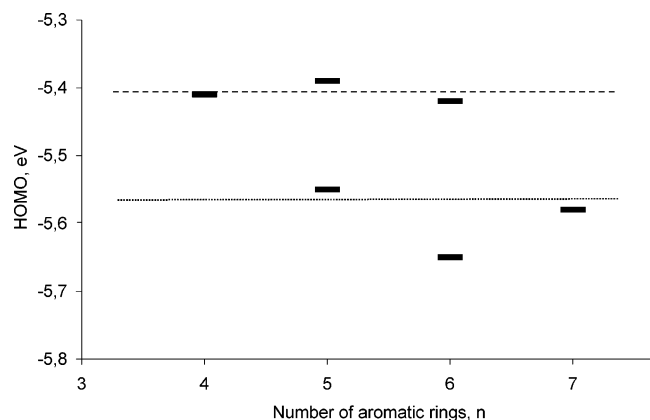


Figure 2. Schematic diagram showing the HOMO levels estimated for the films of oligothiophenes (level 1) and the thiophene–phenylene oligomers (level 2 and below).

between the normal hydrogen electrode and the saturated calomel electrode used by us is -0.24 eV,³² and (3) the jump of the potential on the water–acetonitrile interphase is 0.27 eV.³³ It gives the following

$$E(\text{HOMO}) = -E_{\text{if}}^0 - 4.40 \text{ eV}$$

In fact, it coincides with the formula for the ionization potential given by de Leeuw.³⁴ For a better understanding, the calculated values are presented as a diagram in Figure 2. One can clearly see that the HOMO levels of the oligothiophene films under consideration are concentrated near the HOMO value of -5.40 eV (marked as level 1), almost independently of the number of thiophene rings. Corresponding HOMO levels for the oligomers with one *p*-phenylene ring are shifted by ca. 0.15 eV and located near the value of -5.55 eV (marked as level 2). Insertion of the second *p*-phenylene ring moves the HOMO level further to -5.65 eV for oligomer **3**. It is interesting to note that the same shift of the HOMO level by 0.15 eV was calculated by molecular modeling by Katz et al. for replacing of the central thiophene ring in an α,α' -dihexylquinquethiophene molecule by a *p*-phenylene unit.¹⁷ Comparison of the electrochemical data obtained with the peculiarities in the energy gaps found by optical measurements shows that the insertion of *p*-phenylene rings into oligothiophene molecules mostly influences their HOMO levels, thus increasing their oxidative stabilities.

OTFT Measurements. Semiconducting properties of the thiophene–phenylene oligomers **1–3** were checked by using them as organic semiconducting layers in OTFTs. Charge-carrier mobilities were measured in OTFTs using both top and bottom contact configurations according to a procedure described earlier.^{7,13} A heavily doped silicon wafer was used as the substrate and gate electrode, and a 270 nm thick layer of cross-linked poly-4-vinyl-phenol served as the gate dielectric. Thermally evaporated gold with a film thickness

Table 4. Electrical Characteristics of OTFTs Made from Thin Films of Oligomers **1–3**

compd	contact type	carrier mobility (cm ² /Vs)	threshold voltage (V)	subthreshold slope (V/decade)	on/off ratio
1	top	0.1	2	15	10^2
	bottom	0.3	-5	1.3	10^5
2	top	0.08	-11	8.3	10^3
	bottom	0.08	-8	7.0	10^3
3	top	0.1	-17	5.7	10^4
	bottom	0.4	-13	4.1	10^5

of 30 nm was used for the source and drain contacts. In the top-contact structure, the source and drain contacts were defined using a shadow mask. For the bottom-contact structure, the gold layer was patterned by photolithography and wet etched to define the source and drain contacts. The organic semiconductor layers (30 nm) were deposited by thermal evaporation in a vacuum with a stable deposition rate near 1 nm/min. Substrates were held at room temperature during the deposition. The top-contact OTFTs have a channel length of 130 μm and a channel width of 170 μm . The bottom-contact devices have a channel length of 20 μm and a channel width of 20 μm . To minimize leakage currents and fringe effects, we isolated TFTs under test by scratching a trench around the active device area with a probe tip, thereby removing the organic semiconductor from the trenches (see Figure 1, ref 7a).

All transistors were characterized in air, which confirms their high stability to oxidative doping. From the electrical transfer characteristics, we extracted the parameters such as carrier mobility, subthreshold swing, and on/off current ratio for each device; these are summarized in Table 4. The carrier mobility was extracted from the saturation regime at a drain-source voltage of -20 V and a gate-source voltage of -15 V, meaning that all the oligomers are *p*-type semiconductors. High carrier mobilities of 0.3 and 0.4 cm²/Vs for oligomers **1** and **3**, respectively, were obtained. Compound **2** showed a smaller mobility of 0.08 cm²/Vs, which may be due to a lower degree of molecular ordering, caused by the longer chromophore, as evidenced by the DCS data (Table 1). For the two best semiconductors (oligomers **1** and **3**), the bottom-contact TFTs clearly outperform the top-contact TFTs, with a larger carrier mobility, a smaller subthreshold slope, and a greater on/off current ratio. The same effect was observed for decyl-end-capped oligothiophenes.¹³ This effect was attributed to the formation of the intrinsic barrier by the long decyl groups, separating the dielectric and contact interfaces from the conjugated carrier channel. Such a barrier increases the contact resistance for the top contact TFTs but does not influence the performance of the bottom-contact TFTs. It should be noted that this barrier was not observed for shorter (hexyl and ethyl) alkyl chains.⁷

Figure 3 shows the electrical characteristics of a bottom-contact OTFT made from the 6-ring thiophene–phenylene oligomer **3**. The device has a carrier mobility of 0.4 cm²/Vs, a subthreshold slope of 4.1 V/decade, and an on/off ratio of 10^5 . This is very close to a carrier mobility value of 0.5 cm²/Vs, a subthreshold slope of 3.1 V/decade, and an on/off ratio of 10^5 , measured for its oligothiophene analogue **Dec-6T-Dec**.¹³

(31) Gorevich, Yu. Ya.; Pleskov, Yu. V. *Electrochemistry* **1982**, *18*, 1477.

(32) Dobosh, D. *Electrochemical Constants. (Handbook for Electrochemists)*; Mir Publishers: Moscow, 1980.

(33) Krishtalik, L. I.; Alpatova, N. M.; Ovsyannikova, E. V. *Electrochim. Acta* **1991**, *36*, 435.

(34) de Leeuw, D. M.; Simenon, M. M. J.; Brown, A. R.; Einerhand, R. E. F. *Synth. Met.* **1997**, *87*, 53.

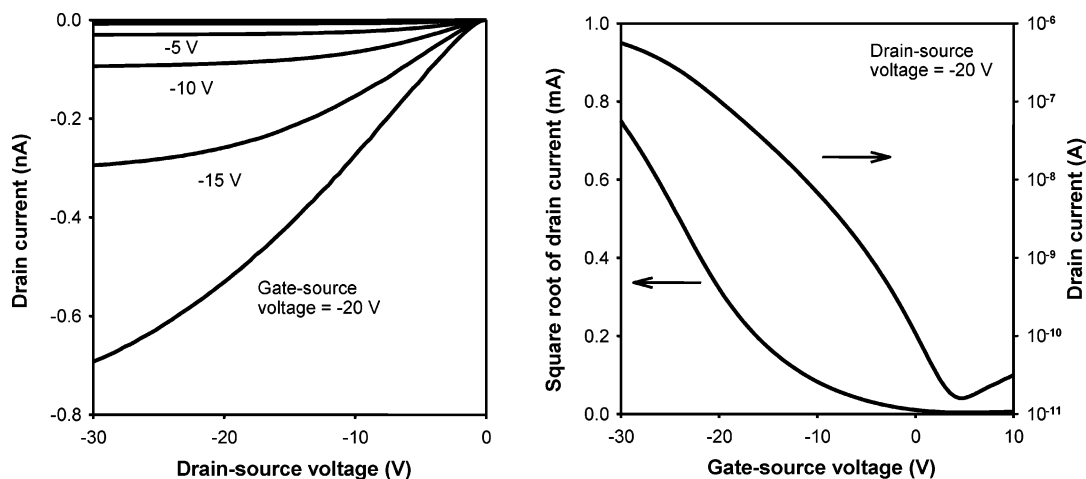


Figure 3. Output and transfer characteristics of bottom-contact OTFT based on oligomer 3.

The potential of these materials for application in organic electronics was demonstrated by the fabrication of integrated circuits (ICs). Five-stage ring oscillators were fabricated on glass substrates as described previously.¹³ Circuits based on oligomers **1** and **3** oscillate with a signal propagation delay between 300 and 700 μ s per stage, corresponding to frequencies of several hundred hertz. It is interesting to note that although oligomer **1** has a somewhat higher mobility than oligomer **3** (0.3 cm²/Vs vs 0.4 cm²/Vs), the faster ring oscillator was obtained from oligomer **1**. This is obviously due to the fact that the performance of the ICs depends not only on the mobility but also on some of the other parameters of the organic semiconductors. One of them is the semiconductor's HOMO level, especially its deviation from the work function of the contact electrodes; the closer the HOMO level of the *p*-type organic semiconductor is to the work function of the electrode, the better. We have used gold contacts, which have work functions: Au (110), -5.37 eV; Au (100), -5.47 eV; and Au (111), -5.31 eV.^{10a} These values are closer to the HOMO level of oligomer **1** (-5.55 eV) than to that of oligomer **3** (-5.65 eV), thus allowing faster charge transfer. This assumption is supported by the fact that much faster ICs, oscillating with a signal propagation delay as short as 30 μ s per stage, were made from **Dec-6T-Dec**, which have a very close mobility value of 0.5 cm²/Vs, but a HOMO level of -5.42 eV that matches well with the IPs of gold.

Conclusions

In summary, we have demonstrated the efficient synthesis of decyl-end-capped thiophene-phenylene oligomers with different numbers and positions of 1,4-phenyl rings within 2,5-oligothiophene conjugated chains, leading to electronic-grade pure semiconducting organic materials. The semiconducting properties of the oligomers were evaluated in organic transistors, which showed that they are *p*-type organic semiconductors with carrier mobilities as large as 0.4 cm²/

Vs and on/off current ratios as large as 10⁵, as well as in integrated circuits (ring oscillators) with stage delays as short as 300 μ s. Although these oligomers possess limited solubility, they are highly crystalline materials, which makes them promising candidates for organic electronic devices prepared by vapor evaporation. Investigation of the optical properties of these oligomers with 5–7 conjugated aromatic rings showed that they have a HOMO–LUMO energy gap ca. 0.2 eV higher than that of the corresponding oligothiophenes. Electrochemical measurements revealed a better oxidative stability of the thiophene-phenylene oligomers compared to that of their oligothiophene analogues. Estimation of the HOMO levels of the oligomer films showed that for α,α' -didecyloligothiophenes with 4–6 conjugated thiophene rings, it is almost independent of the oligomer length and is close to a value of -5.40 eV. Inclusion of one *p*-phenylene ring in a conjugated oligothiophene chain shifts this value to approximately -5.55 eV, whereas the second *p*-phenylene ring shifts the value 0.10 eV further.

The current study indicates that combining 2,5-thiophene and *p*-phenylene units in the conjugated oligomer is a promising approach for the creation of new stable semiconducting materials with high charge-transport mobility and good device performance. It allows for tuning the energy gap as well as the oxidation stability of the organic semiconductors. The presence of long alkyl chains in such oligomers improves their molecular ordering, thus positively influencing their semiconducting properties.

Acknowledgment. The authors thank Dr. H. van Well, Dr. R. Friebe, Dr. J. Wesener (Bayer AG, BSD-ZA), and their co-workers for help in characterizing the new materials synthesized. S.A.P. thanks H. C. Starck GmbH, the Russian Science Support Foundation, and the Russian Foundation for Basic Research (Grant 04-03-32294) for financial support.

CM052210M